XMaS

NEWSLETTER

2016

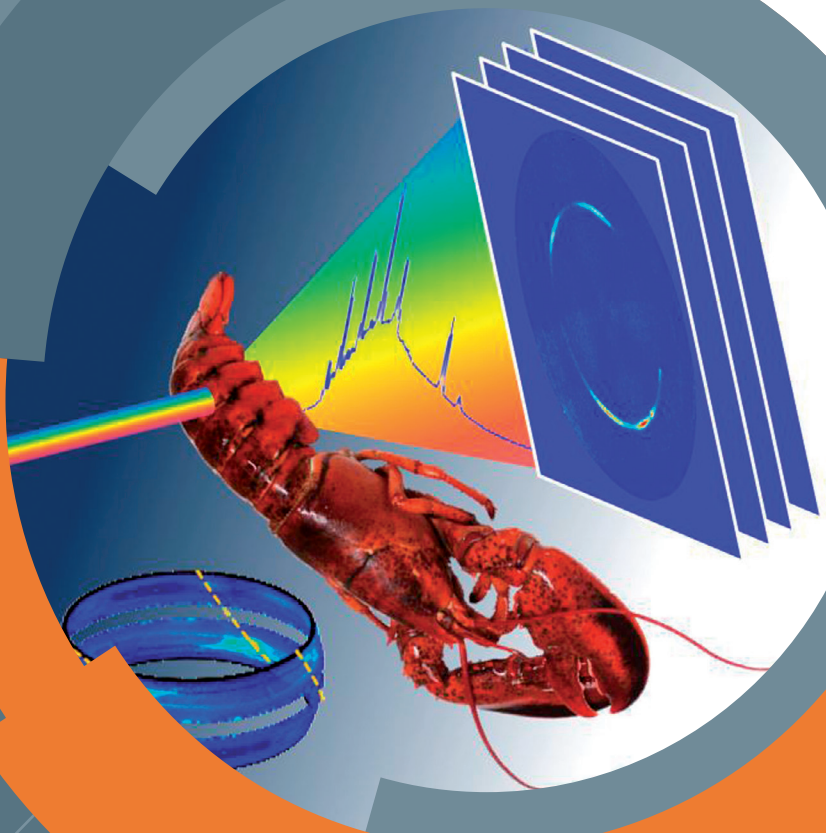

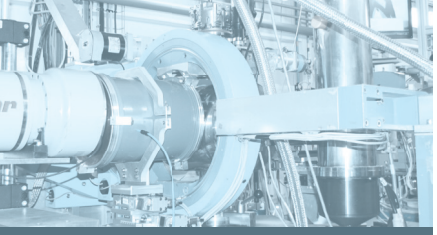

XMaS News

CONTENTS

On the cover: *When a white x-ray beam provides 3D crystallographic information in texture analysis (p. 11).*

As can be seen in the enclosed highlights, the scientific output remains as diverse as ever with topics covering a wide range of materials science. As usual we are indebted to the evolving user community for their continuing support. Over the past operational year there were 90 individual user visits to the synchrotron beamline from over 44 research groups (33 from the UK and a further 11 from their international collaborators). Of these visits, 32 were from new users with 52 being either postdoctoral researchers or students. In addition to the beamline, we provide access to offline facilities which include a magneto-transport laboratory for material characterisation under electric and magnetic fields without x-rays, as well as a high brightness x-ray source for x-ray diffraction and reflectometry. For the x-ray laboratory there were a total of 15 user visits covering 11 proposals with 4 proposals being handled as remote, or "mail-in" experiments handled by the on-site team. We encourage you to consider applying to use the additional facilities through the online access mechanism described on the web page (www.xmas.ac.uk).

The scientific highlights presented herein exploit the full capabilities of the beamline and the sample environments we have developed. Our staff are always happy to explore possible new sample environments or metrology tools. We have recently added a new large area Ketek detector to the detector suite and continue to develop bespoke sample environments. We are also concentrating our efforts on data reduction, visualisation and processing, particularly to facilitate the non-expert synchrotron user. As always, we would welcome any feedback you may have in how we can support your research more fully and what developments you would like to see coming to XMaS.

We continue to be engaged with outreach and this year we ran "The XMaS Scientist Experience" for the second time. 16 winners from around the country were taken on a trip to the ESRF where they participated in the Synchrotron@School program (**Fig. 1**) and visited a number of beamlines around the ESRF (including XMaS). The general aim of the activity is to encourage young women to consider careers in STEM* by showing them possible job opportunities and introducing them to inspirational role models. The trip

Fig. 1: *Hands-on experiment during the ESRF Synchrotron@School programme.*

received a lot of attention on social media (@XMaSSchoolTrip) and we thank all involved in making it so successful.

XMaS has now been supporting users for nearly 20 years. We normally engage with our user community through the annual user meeting, which this year was held at the University of Warwick in May 2016. To celebrate the 20 years of operation we will be hosting an extended user meeting at the ESRF on the 20-21 September 2017 – almost to the day we started user operations in 1997. Further details and registration can be found on the web page (www.xmas.ac.uk/impact/meetings/xmas_20/). We hope to welcome as many of you as possible to the meeting to both look back at how XMaS has changed and to hear about the current research activities.

We also continue to look towards the future. Funding of a one year extension to take user operations up to the ESRF shutdown at the end of 2018 is under final negotiation. In addition, we are planning a significant refresh and upgrade of both hardware and software to align the beamline to the new opportunities of the new ultra-low emittance storage ring. Further details can be found on page 3. The new source and beamline will allow us to support more users from across the materials science community.

Finally, we would like to announce that Didier Wermeille is now the "beamline responsible" and guiding the team in France. We thank Simon Brown for his many years of service in this role. Sean McMitchell has moved on after the Nanostrain project came to an end and we wish him success in his future career. We also welcome Harry, Kayleigh's new born son to the XMaS family!

Chris Lucas, Tom Hase and Malcolm Cooper

*STEM: Science, Technology, Engineering and Mathematics

EPSRC Engineering and Physical Sciences Research Council

WARWICK THE UNIVERSITY OF WARWICK

UNIVERSITY OF LIVERPOOL

XMaS post 2018

After the successful delivery of the first phase of the upgrade programme in the period 2009-2015, the ESRF launched the Extremely Brilliant Source (EBS) project **[1]**. This ambitious project involves the design and implementation of a new ultra-low emittance storage ring to be constructed and commissioned within the existing storage ring tunnel. When completed in 2020, the ESRF will be one of the brightest synchrotron facilities in the world. The upgrade is particularly well-timed for the XMaS facility which is also in need of updates and upgrades after nearly 20 years of user operation. Following consultation with our users we will upgrade our current source to a high field 0.86 T short bending magnet. We are in the final stages of compiling a technical design review which, when completed, will be posted online.

EBS opportunities and extended capabilities

The new lattice will have a significant impact on BM28. Geometrically the source will move ~3 m upstream. Its position in the upgraded lattice will ensure a more stable and a better defined electron orbit. The higher magnetic field of the source and concomitant higher critical energy increases the available flux at energies above 20 keV by several orders of magnitude. Extensive SHADOW calculations, incorporating realistic estimates for aberrations arising from the optical elements, have enabled us to model the new source characteristics as functions of both energy and focal length. **Fig. 2** shows the results of these calculations at different positions close to the focal point of the new mirror. At the focus, the beam is significantly smaller and well defined with a spot size of ~50 (H) x 80 (V) µm, an order of magnitude smaller than our current beam profile (300 x 600 µm). As the source point will move, aberrations in the beam shape are evident at the current diffractometer position. We will therefore extend the experimental hutch and move our diffractometer to maintain our current magnification and minimise any beam aberrations. A hutch extension of 4 m will also allow additional beam defining and conditioning elements to be incorporated, increasing operational efficiency and allowing rapid switching between experimental configurations.

Post EBS upgrade, the beamline will have more than an order of magnitude gain in usable flux density at conventional energies for most of the experiments as well as access to higher energies.

As the majority of experiments performed on XMaS require a small footprint/small angular divergence the more brilliant source increases usable flux for most users by an order of magnitude or more. Further increases in the S/N ratio are derived from the reduced background as the beam is no-longer being defined close to the sample.

For the user community, the newly upgraded beamline will enable higher sample throughput, open up studies of weakly scattering systems as well as emergent phenomena more generally. The core capabilities of the beamline will remain unchanged, but the high energy and brightness will allow new insights into quantum critical behaviour as well as facilitating studies of confinement and proximity in magnetic and superconducting materials. Advances in simultaneous studies allow the direct correlation of functional properties with structure at frequencies up-to 1 MHz. Newly combined (GI)-SAXS*/WAXS* and XRR* metrologies allow the structure to be measured across a wide range of length scales simultaneously. The higher brightness will enable more systems to be studied *in-operando* and on relevant timescales allowing the study of ionic migration in battery systems and photovoltaics. The well-defined and small beam will facilitate experiments on small samples or on localised regions of larger samples. Structural studies will be more spatially resolved enabling individual domains and their temporal evolution to be studied under external stimuli. Such activities provide new insights into phase transitions and the emergence of new functional properties.

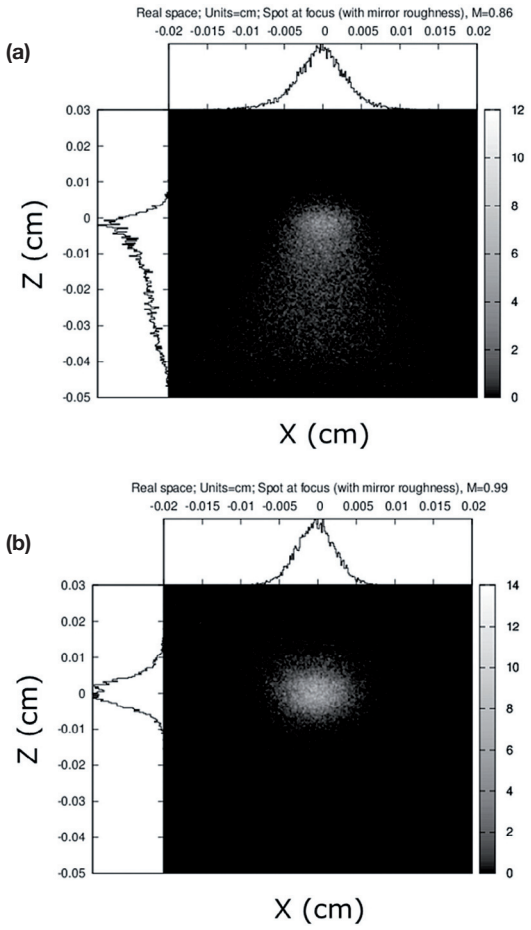

Fig. 2: *Beam shape at the current diffractometer position, magnification=0.86* ***(a)*** *and at a magnification of 0.99* ***(b)*** *Calculations performed using 8 keV radiation.*

New mirrors will allow continuous and tuneable energy operations from 2.035 to ~40 keV. This transforms studies of new catalysts and green chemistry more generally – being unique in probing the same sample volume across this entire energy range and within the same sample environment. Thus,

reactions can be followed on a site-by-site basis and in real time. An upper energy of ~40 keV will allow experiments to access the K edges of the rare earths as well as enabling new studies on the L edges of the transuranic elements. The higher energies also facilitate experiments on buried interfaces in more complex sample environments. Studies of solid-liquid interfaces relevant to electrochemical processing become possible. The smaller horizontal divergence enables the front-end Be window to be thinned further, increasing the useable flux at low energies. Finally, the new lattice will greatly facilitate polarisation studies due to the better defined beam position and more efficient phase retarders leading to the development of new polarisation studies such as SAXS/WAXS from chiral systems.

We are excited about the opportunities that the EBS project brings to XMaS and welcome comments from our user community as we refine and develop the technical design study. We would especially encourage engagement with us on any new sample environments that you need to exploit the enhanced capabilities of XMaS post upgrade and look forward to hearing from you.

[1] www.esrf.fr/about/upgrade

* See glossary p.5 for definition.

WORKSHOPS

X-ray & Neutron Scattering in Multiferroic and Ferroelectric Materials Research IV

M.G. Cain, Electrosciences Ltd, Farnham, Surrey, and R.J. Cernik, University of Manchester, M13 9PL,UK.

markys.cain@electrosciences.co.uk
r.cernik@manchester.ac.uk

The X-ray *& Neutron Scattering in Multiferroic and Ferroelectric Workshops* comprise a series of one day meetings **[1]** co-organised by the Smart Materials & Systems Committee of the UK's Institute of Materials, Minerals and Mining **[2]**, Electrosciences Ltd **[3]** and the XMaS beamline **[4]**. Our 4th workshop was held at IOM3 London headquarters on 3rd November 2016. The focus of this event was on scientific advances made in these materials systems through the application of advanced x-ray and neutron techniques. The meeting had talks from Judith Driscoll (University of Cambridge), Federica Fabrizi (DLS), Paolo Radaelli (University of Oxford), Pascal Manual (ISIS), Dmitry Chernyshov (ESRF/Swiss Norwegian beamline), Peter Finkel (US Naval Research Labs), Semen Gorfman (University of Siegen, Germany) Markys Cain (Electrosciences).

The meeting culminated in an informal yet captivating wrap up session chaired by Bob Cernik. Highlights included (i) the IT challenges associated with the very large datasets expected from the emergence of 2D detectors and 3D reciprocal mapping images (where visualisation strategies need developing), (ii) the necessity to explore the complex perovskite relaxor ferroelectric materials with ever smaller x-ray beams (beam size down to a few 10s of nm is available at nanoprobe beamlines e.g. ID16 at ESRF and 26 ID-C at APS), (iii) improving the temporal resolution in dynamic studies using x-ray synchrotrons (such as the TimePIX Diamond imaging system), and (iv) *in-situ* measurements of structure, magnetic field, electric field, stress, temperature and pressure, often needed by materials scientists and increasingly by chemists and electrochemists.

Professor Cernik of Manchester University has spent a year on secondment at ESRF and says "*Multiferroic and ferroelectric materials offer the opportunity for many new types of devices - from ultralow magnetic field sensors to new types of multiple state memories. Much has been learnt on these materials via diffraction and spectroscopy techniques through synchrotron and neutron scattering combined with other methods, including bulk and thin film metrology and atomistic modelling".*

[1] www.xmas.ac.uk/impact/past_meetings/multiferroics/
[2] www.iom3.org
[3] www.electrosciences.co.uk
[4] www.xmas.ac.uk

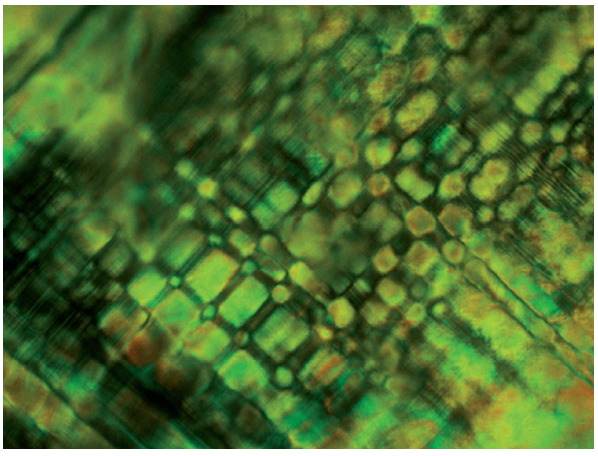

Fig. 3: *Image of domains in single crystal piezoelectric materials: image size about 120 µm across. Copyright HMSO.*

Catalysis@XMaS

G. Sankar, University College London, Department of Chemistry, London WC1H OAJ, UK

g.sankar@ucl.ac.uk

In the modern era, catalysis has become a major force in the chemical industry. Almost 85% of the materials we use in daily life have undergone some kind of catalytic process. Without our knowledge, catalysis is present everywhere. For example, nylon is used widely for making textiles. The molecules to make nylon are produced through a series of catalytic processes starting from benzene converting to cyclohexane to hexanedioic acid followed by a reaction with hexamethylene diamine to form nylon 6,6. Another example, which benefits our life and environment is the use of auto-exhaust catalysts to convert toxic gases such as CO, NO and unburnt hydrocarbon to benign gases.

While catalytic processes are widely carried out, it has been realised that understanding the electronic and geometric structure of the active site is vital to establish the structure-function relationships, which will enable the design of new and better catalysts. With the introduction of synchrotron radiation x-ray absorption spectroscopy (both XANES* and EXAFS*) has become a very popular technique for the study of catalysts. This technique is element specific and does not depend on the presence of long-range order. Furthermore, elements with low concentration can be investigated relatively easily (see **Fig. 4**).

Whilst a range of beamlines offer both *in-situ* and *ex-situ* methods to study catalytic materials, many of them operate between 4 and 30 keV, which restricts the type of elements and absorption edges that may be investigated. This energy range mainly allows the study of elements after titanium in the periodic table. Only a limited number of beamlines are available for studies of elements with an atomic number below titanium. Moreover, study of the L-edges of the second row (*2d*) transition metals (ca between 2 - 5 keV) can be more valuable as it allows us to probe directly the *d*-states. With a minimum energy of 2.4 keV (and down to 2.035 keV after the ESRF upgrade), XMaS provides an ideal opportunity to investigate catalytic materials that are normally difficult to study in many other beamlines. For example, investigation of S and Cl K-edges can provide information on the nature of the ligands and how they are bonded to cations. Similarly, L-edges XAS of cations such as Nb, Rh, Pd, Ag, etc… is of considerable interest to the catalytic community (e.g. **Fig. 4b**). The different methods of detection available at XMaS, in particular

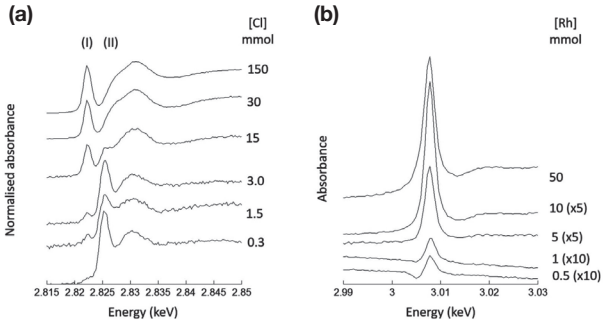

Fig. 4: *An example of XMaS study demonstrating the viability of experiments that will benefit the catalytic community.* ***(a)*** *Normalized Cl K-edge XANES and* ***(b)*** *Rh L3 edge XANES absorbance (not normalised) derived from aqueous RhCl3 solutions as a function of Cl. In* ***(b)****, scaling factors, to aid comparison over the range of concentrations are given in parentheses. Taken from* ***[2]****.*

transmission and fluorescence modes, can also significantly benefit this community. In addition to the XAS* capability offered at XMaS, it is possible to combine different methods, e.g. XAS/SAXS, XRD*/SAXS and XRD/XAS but also XRD/XAS/SAXS, which is again a distinct advantage to the catalytic community.

Catalysis Hub **[1]** located at Harwell Campus brings together several researchers in the UK to advance catalytic science. Scientists who are linked and working at this site exploit synchrotron radiation techniques extensively to characterise their catalysts using a range of techniques, in particular XAS, XRD and SAXS. This community will significantly benefit from using XMaS, in particular for energies below ca 5 keV. Although B18 at DLS can be used, XMaS will complement B18 and support users for two main reasons: (i) unique combination of SAXS/XRD/XAS method at XMaS and (ii) oversubscription of B18. In summary, XMaS offers a range of unique capabilities that will benefit the catalytic community in the UK.

Read also the short review article by M.A. Newton and P. Thompson (p. 6) and the highlight of N. Yokota et al. (p. 14) on XAS measurements.

[1] http://www.ukcatalysishub.co.uk/

[2] P.B.J Thompson *et al.*, J. Synchrotron Rad. 22, 1426 (2015).

***Glossary:**

EXAFS: Extended X-ray Absorption Fine Structure
SAXS: Small Angle X-ray Scattering
SEM: Scanning Electron Microscopy
XANES: X-ray Absorption Near Edge Spectroscopy
XAS: X-ray Absorption Spectroscopy
XRD: X-ray Diffraction
XRR: X-ray Reflectivity
WAXS: Wide Angle X-ray Scattering

Soft x-ray spectroscopy for materials chemistry comes online

M.A. Newton, University of Warwick, Coventry CV4 7AL, UK and P. Thompson, XMaS.

p.thompso@esrf.fr
manewton68@gmail.com

Recent work **[1]** has shown that XMaS possesses considerable potential as a high flux resource for XAS* in the 2-4 keV regime, an energy range that is relatively under resourced for users. The K-edges of P, S, Cl, and K as well as the L_3 edges of transition such as Ru, Rh, Pd and Ag, all exist in this energy window and all are of significant interest in catalysis as well as numerous other chemically oriented areas. However, in such areas one must go beyond simply being able to measure XAS spectra. One needs to present the sample and study it as it is experiencing environments relevant to its function, be they flowing gases and at elevated temperature, or when a liquid phase is required for function; the latter being almost ubiquitous in the fine chemical synthesis that underpins the pharmaceutical industry. XMaS is therefore now working with different UK based research groups to provide the resources that can realise such studies and specifically in the arena of liquid-solid catalysis that is both very important but relatively understudied using x-ray methods; this is especially the case in the lower energy regime where restrictions upon windowing materials and sample presentation can be challenging.

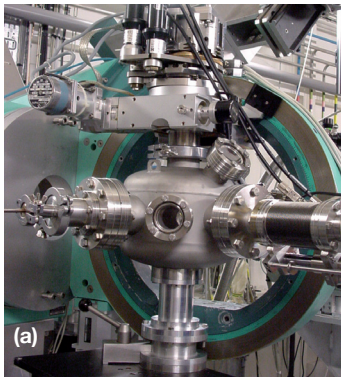

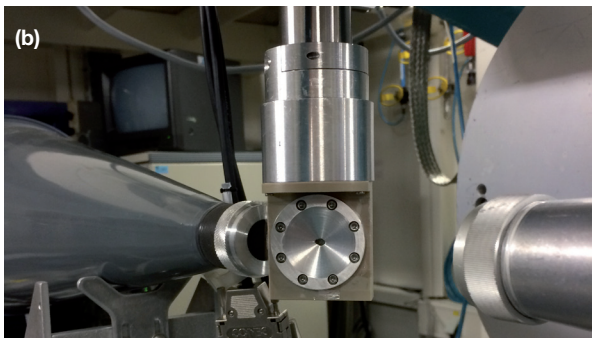

Fig. 5: (a) *XMaS chamber for* in-situ *soft XAS.* ***(b)*** *Insertable sample environment for* in-situ *study of liquids and liquid-solid systems using fluorescence yield XAFS in the 2-4 keV range.*

A modular vacuum chamber system (**Fig. 5**) has been implemented to house new sample environments (**Fig. 5**) designed specifically for such studies. *In-operando* measurements using Cl, S, and K K, and Rh and Pd L_3 edges, have already been demonstrated to provide much insight in understanding deactivation processes in $CpIrCl_2$ based transfer hydrogenation catalysts **[2]**. They have also been used to understand the roles that Cl may have in affecting the development and behaviour of conventionally supported Pd catalysts **[3]** and polymer encapsulated Pd systems; the latter are widely used in fine chemical synthesis **[4]**. These studies, allied to fast EXAFS* measurements made at beamlines such B18 at DLS and SNBL at ESRF, have shown that Cl can have a variety of effects on Pd catalysts that depend upon the state of the Pd present in the system and the synthesis process used. For example we have revealed that the use of chlorinated solvent in the production of commercially available and widely used polymer encapsulated Pd catalysts, can have a very significant effect on how the Pd develops under flowing solvents such as aqueous ethanol **[4]**.

Cl K-edge XANES* shows that Cl (derived from the chlorinated solvent during the encapsulation process) can become trapped along with the Pd precursors used, and that much of this retained Cl can coordinate directly to the Pd^{II} present in the starting catalyst. The result is a very effective suppression of the formation of catalytically active Pd^{O} nanoparticles even under heating to 353 K in aqueous ethanol. In samples where Cl has not been retained Pd^{O} nanoparticles are formed by simply wetting the sample at ambient temperature. This application of Cl and Pd L_3 edge XAFS* using these new facilities at XMaS has therefore highlighted a fundamental role that Cl may play in the development of supported and encapsulated catalysts. Further, it has shown that elements of the production of polymer encapsulated catalysts system might be best modified such that a compositionally more consistent, Cl-free, and facilely reducible product may result.

[1] P.B.J Thompson *et al.*, J. Synchrotron Rad. 22, 1426 (2015).

[2] G.J. Sherbourne *et al.*, J. Am. Chem. Soc. 137, 4151 (2015).

[3] J.B. Brazier *et al.*, Catal. Struct. React. (in press), DOI: 10.1080/2055074X.2016.1267296.

[4] M.A. Newton *et al.*, to be published.

* See glossary p.5 for definition.

Surface and interface atomic structures of electrodeposited Co films on Au(111)

C.A. Lucas, F. Maroun, N. Sisson, P. Thompson, Y. Gründer, R. Cortes and P. Allongue – for more information contact C.A. Lucas, Department of Physics, University of Liverpool, Liverpool L69 7ZE, UK.

clucas@liv.ac.uk

Ultrathin magnetic layers often present perpendicular magnetic anisotropy (PMA), a phenomenon of strong interest for high density data storage and, more generally, spin electronics. PMA is characterised by a critical thickness t* of the ferromagnetic film at which the magnetisation easy axis switches from out of plane to in–plane. It arises from the film interfaces, the film structure and the possible presence of strain. Consequently, PMA is very sensitive to the growth method of the magnetic layer. In this respect electrodeposition has been shown to be a competitive method for preparing epitaxial films and nanostructures over large surface areas. Initial studies demonstrated that Co/Au(111) layers can be grown from a modified Watts bath and the method has been extended to produce thin Au/Co bilayers deposited on Au(111) with a critical thickness t* of ~ 8-10 monolayers (ML). This is comparable to that found for Co films grown by molecular beam epitaxy (MBE) in ultra-high vacuum (UHV). In addition, *in-situ* magnetic characterisation, using the Magneto Optical Kerr Effect (MOKE) revealed that the value of t* can be modified by adsorbing small molecules (like carbon monoxide) onto the surface of the cobalt film that is in contact with an electrolyte. Very recently, it was further reported that the electric field at the electrochemical interface can reversibly alter the magnetic properties of the Co films. This magneto-electric effect is becoming very topical as it opens a route to new magnetisation switching methods in memory or storage devices.

Since PMA is sensitive to the structure and may, in particular, be affected by strain, we undertook an *in-situ* structural characterisation of Co/Au(111) layers in contact with an electrolyte. **Fig. 6** shows the x-ray scattering data (specular crystal truncation rod, CTR) measured for a 2 ML thick Co film covered by CO. The CTR is clearly different from that calculated for a bare Au surface (dotted blue line) as it exhibits oscillations with a well-defined period between the Au Bragg reflections at L=0, L=3 and L=6, and these oscillations are consistent with a Co film thickness of ~2 ML. A layered model shown schematically in **Fig. 6** was used to fit the data. The results show that the Co film is bi–dimensional with 2 ML thick Co islands covering ~80% of the Au(111) surface. The measurements also indicated that there was ordering in the electrolyte side of the interface.

The deposition of the Co layer induces a modified Au(111) surface reconstruction with an isotropic in–plane compression of 2% of the topmost Au atomic plane. The adsorption of CO onto the surface of the Co film has no significant impact on the in-plane structure of the Co layer. Furthermore, the influence of the applied potential on such a CO-covered Co film indicated that only the electrolyte layering is affected by the potential while the Co film structure remains unaltered. This suggests that the strong magnetoelectric coupling observed at CO-covered Co/Au(111) films is not due to structural rearrangement of the Co layer but to the modification of the Co surface electronic structure. Full details of the XMaS experiment are reported in reference **[1]**.

[1] C.A. Lucas *et al.*, J. Phys. Chem. C 120, 3360 (2016).

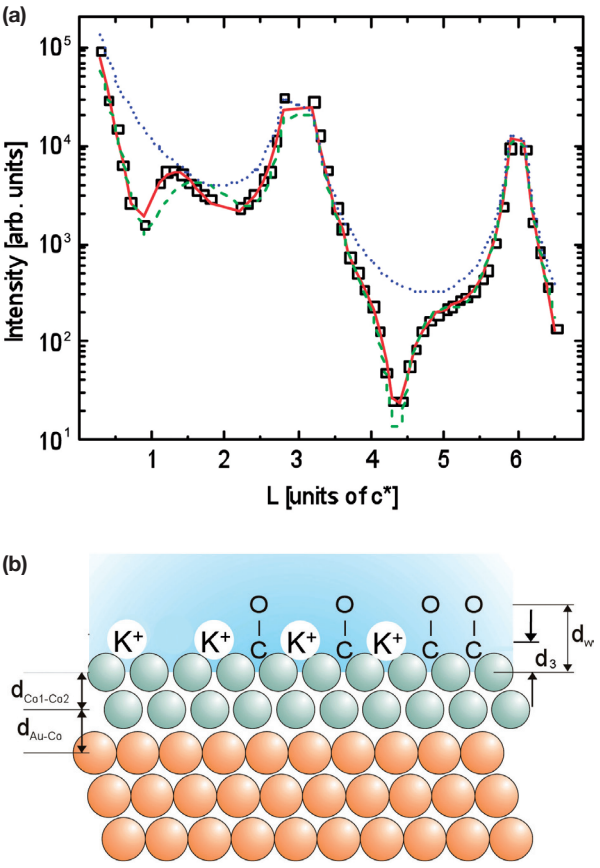

Fig. 6: (a) *Specular CTR data, (0, 0, L), for a 2 ML Co film after saturation of the electrolyte with CO. The solid red line is a fit to the data.* ***(b)*** *Schematic model of the layering in the Au/Co/electrolyte system determined from the CTR data.*

X-ray resonant magnetic reflectivity for spin caloritronics

T. Kuschel, P. Bougiatioti, C. Klewe – for more information contact T. Kuschel, Center for Spinelectronic Materials and Devices, Department of Physics, Bielefeld University, 33615 Bielefeld, Germany.

tkuschel@physik.uni-bielefeld.de

Spin caloritronics is quite a young research field exploring the interaction between thermal transport and spin currents **[1]**. The most important effect in this area is the spin Seebeck effect (SSE) that describes the generation of a spin current in a ferro- or ferrimagnetic material (FM) by a thermal gradient **[2]**. It is analogous to the classical Seebeck effect that describes the generation of a charge current via a thermal gradient. The SSE is a promising candidate to recycle waste heat in spintronic devices for the creation and manipulation of spin currents **[3]**.

A common way to detect these thermally induced spin currents is the use of an adjacent heavy metal material with large spin-orbit coupling such as paramagnetic Pt. The so-called inverse *spin* Hall effect **[4]** in Pt converts the entering spin current into a transverse charge current that can easily be measured. However, Pt is close to being magnetic (close to the Stoner criterion) and therefore can easily become magnetic when being in close proximity to a FM. This magnetic proximity effect (MPE) at the interface can create parasitic effects **[5]**, which can hamper the spin current detection in Pt.

We used synchrotron x-ray resonant magnetic reflectivity (XRMR) **[6, 7]** in order to identify or exclude MPE in Pt on several FMs. The concept of XRMR is illustrated in (**Fig. 7**). At XMaS, the circularly polarised x-rays incident on the sample were produced using a single diamond phase-plate. The magnetic field was applied in the plane of the sample. Here, the specular x-ray reflectivity (XRR) (**Figs. 8a** and **c**) and the asymmetry ratio of the XRMR curves (**Figs. 8b** and **d**) were modelled for Pt/Fe bilayers having two different thicknesses. Due to the magnetic state of Pt at the interface, the magneto-optic parameters of Pt change slightly for either opposite magnetic field directions or opposite helicities **[8,9]**. This can be identified in the XRR curves by varying the scattering angle θ and thus the scattering vector q. A clear MPE (~±2% asymmetry ratio independently of Fe thickness) can be found in these Pt/Fe systems. Further simulations using different depth profiles of the spin polarisation in Pt can be found in Refs **[7-9]**.

As we explored SSE in the FM insulator $NiFe_2O_4$ (NFO) **[10]**, we also used XRMR at XMaS to investigate MPE in Pt/NFO bilayers **[9]** but did not find any non-zero asymmetry ratio in these samples. Thus, no parasitic MPE-based effects in Pt disturb our detection of the thermally generated spin currents in NFO.

[1] G.E.W. Bauer *et al.*, Nat. Mater. 11, 391 (2012).
[2] K. Uchida *et al.*, Appl. Phys. Lett. 97, 172505 (2010).
[3] K. Uchida *et al.*, Proc. IEEE 104, 1946 (2016).
[4] E. Saitoh *et al.*, Appl. Phys. Lett. 88, 182509 (2006).
[5] S.Y. Huang *et al.*, Phys. Rev. Lett. 109, 107204 (2012).
[6] S. Macke and E. Goering, J. Phys.: Condens. Matter 26, 363201 (2014).
[7] T. Kuschel *et al.*, Phys. Rev. Lett. 115, 097401 (2015).
[8] C. Klewe *et al.*, Phys. Rev. B 93, 214440 (2016).
[9] T. Kuschel *et al.*, IEEE TM 52, 4500104 (2016).
[10] D. Meier *et al.*, Phys. Rev. B, 87, 054421 (2013).

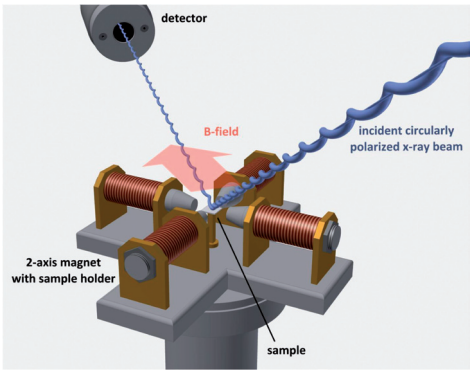

Fig. 7: *Concept of XRMR: Circularly polarised x-rays are reflected from a magnetised sample. For each scattering angle θ either the magnetic field or the helicity of x-rays is switched.*

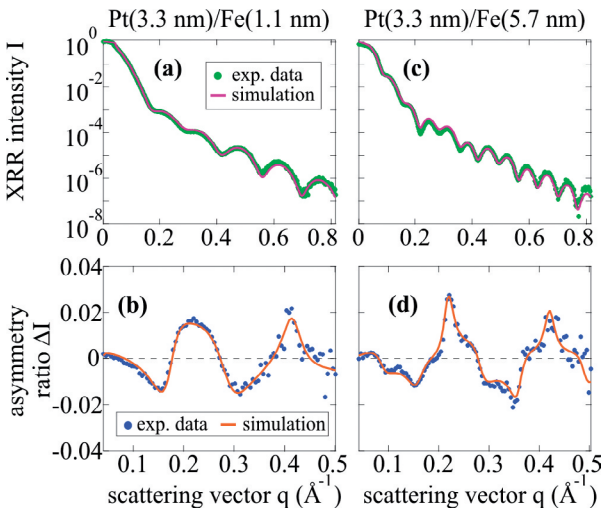

Fig. 8: (a, c) *Specular XRR and* ***(b,d)*** *asymmetry ratio measured across the Pt L_3 edge (11.56 keV) for Pt/Fe bilayers sputtered on $MgAl_2O_4$ substrates. Taken from* ***[9]****.*

Defining the impact of paternal diet on offspring bone health

A.J. Watkins, S. Sirovica, O. Addison, R.A. Martin – for more information contact A.J Watkins - Aston Research Centre for Healthy Ageing, Aston University, Birmingham B4 7ET, UK

a.watkins1@aston.ac.uk

The risk of developing diseases such as osteoporosis, heart disease and obesity are associated with adult life-style factors such as diet, exercise and smoking. However, human and animal model studies have revealed that our development prior to birth can be just as important for adult health. Studies manipulating maternal diet during pregnancy, reveal that being significantly heavier or smaller at birth can increase the risk of developing osteoporosis, heart disease and obesity in adult life **[1]**. While we understand the impact of a poor maternal diet for the long-term health of her offspring, the significance of a fathers' diet has been relatively overlooked.

We fed male mice either a control normal protein diet (NPD: 18% protein) or a sub-optimal low protein diet (LPD: 9% protein) prior to mating with NPD fed females for the generation of offspring **[2]**. For this study, we analysed offspring development in late gestation (day 17, term being day 19), representing a time of maximal fetal growth and skeletal development. Using micro-tomography (μ-CT) scanning, we observed that fetal offspring from LPD fed males were significantly heavier with larger skeletal volumes when compared to offspring from NPD fed males (**Fig. 9a**).

To determine the impact of a paternal LPD on bone structure we used XRD* on XMaS to obtain hydroxyapatite crystallographic lattice parameters (**Fig. 9b**). Taking multiple line transects across fetal humerus and femur bones, we observe significantly increased *a=b* (16° scattering angle) and c lattice (13° scattering angle) parameters in LPD offspring bones **(Fig. 10)**. Such changes indicate either compositional variation in the apatite crystallites or crystallographic differences relative to the crystallite particle morphology. However, the ratio of the unit cell parameters *c/a* remained similar between NPD and LPD diets (0.707). Therefore, these data indicate lattice changes attributable to growth-rate effects rather than phenomena associated with bone maturation where a-lattice parameters decrease whilst the c-lattice remains constant **[3]**.

These findings indicate previously undescribed perturbation of bone growth with disruption of "normal" mineralization at the ultrastructural level. Although the exact physico-chemical mechanisms are not yet elucidated there are clear implications for bone function. Further studies will determine whether our results represent a delay in ossification or a more permanent disruption of bone tissue.

[1] K.D. Sinclair *et al*., Reprod. Fertil. Dev. 26, 99 (2013).

[2] A.J. Watkins *et al*., Am. J. Physiol. Heart. Circ. Physiol. 306, H1444 (2014).

[3] R.G. Handschin *et al*., Bone 16, S355 (1995).

* See glossary p.5 for definition.

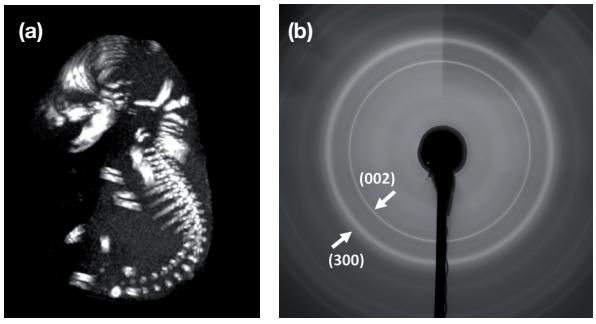

Fig. 9: (a) *Representative μ-CT image of a whole mouse fetal skeleton.* ***(b)*** *Representative XRD diffraction pattern showing typical hydroxyapatite 002 and 300 planes.*

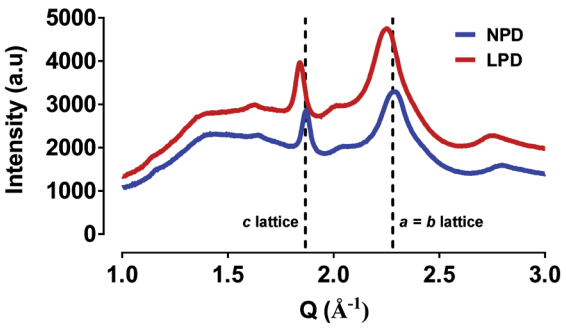

Fig. 10: *XRD spectra for NPD and LPD fetal humerus and femur hydroxyapatite.*

Teeth as a window into hard tissue disruption caused by inherited metabolic disorders

M. Al-Jawad, M.A Khan, O. Addison, A. James, C.J. Hendriksz - for more information contact M. Al-Jawad, Institute of Dentistry, Queen Mary University of London, London E1 4NS, UK.

m.al-jawad@qmul.ac.uk

Dental enamel is a highly mineralised tissue, therefore like bone can undergo metabolic disturbances during tooth developmental stages that can lead to disorientation of enamel crystallites and defects in enamel structure. When this occurs in *amelogenesis imperfecta* for example, it is important to understand the changes happening in the enamel structure at multiple lengthscales in order to relate them to the underlying genetic mutation and thus aid better dental clinical treatment **[1]**.

However, when enamel disruption exists as part of a musculo-skeletal condition that also affects bone tissue, then enamel becomes useful as a more readily accessible mineralised tissue. Additionally, since enamel does not remodel, it offers a snapshot in time of disturbance at a particular developmental stage that can be related to bone development. In this context, we studied the dental enamel from patients affected by inherited metabolic disorder *mucopolysaccharidosis* (MPS) using XMaS.

MPS is a rare metabolic disorder with a prevalence of approximately 1 in 100,000. There are seven subtypes of MPS, and this study focussed on MPS I (Hurler syndrome) and MPS IVA also known as Morquio's syndrome. In both types of MPS, deficiency of an enzyme responsible for the breakdown of glyscosaminoglycans (GAGs) results in a build-up of GAGs in all cells. Clinically the conditions manifest after infancy and are associated with severe skeletal abnormalities, restrictive lung disease, impaired endurance, hearing impairment, and aortic valvular disease.

Samples used in this study were deciduous maxillary central incisors which were collected with ethical consent from individuals affected by MPS I and MPS IVA, and from healthy type-matched control individuals. Samples were cut labio-lingually into longitudinal sections of 0.5 mm thickness in order to carry out 2D synchrotron XRD* and complementary SEM* **[2]**. 2D mapping XRD was carried out on XMaS at 15 keV with a 150 x 150 μm beamspot. The azimuthal variation in intensity around the Debye ring of the (002) Bragg reflection present in the diffraction images was used to determine the degree of texture in enamel, where low values of FWHM represent high preferred orientation and vice versa. The FWHM values for all the diffraction images were assembled to create 2D spatial texture maps (**Fig. 11a**).

In healthy enamel, there is high crystallite orientation at the incisal surface and an organised microstructure, which persists to some degree along the labial and lingual sides **[2]**. In contrast, the enamel affected by MPS IVA shows significantly lower crystallite orientation and microstructural organisation at the incisal surface, and very little organisation at the cervical tip (**Fig. 11**) **[2]**. The loss of prismatic structure, the low preferred orientation and the thinner enamel layer indicate disruption at the secretory stage of enamel formation. This was supported by the earlier observation of poor integration of the tissues at the enamel-dentine junction **[3]**.

In summary, MPS affected deciduous enamel presents with low crystallographic preferred orientation indicating that GAGs accumulation plays an important role in loss of normal enamel structural hierarchy, most likely occurring at the secretory stage. By understanding the stage in which disruption in enamel occurs we can inform the appropriate timings of enzyme replacement therapies for patient benefit.

[1] S. Siddiqui *et al*., J. Dent. Res. 95, 580 (2016).
[2] M.A. Khan *et al*., Micron 83, 48 (2016).
[3] M. Al-Jawad *et al*., J. Dent. 40, 1074 (2012).

* See glossary p.5 for definition.

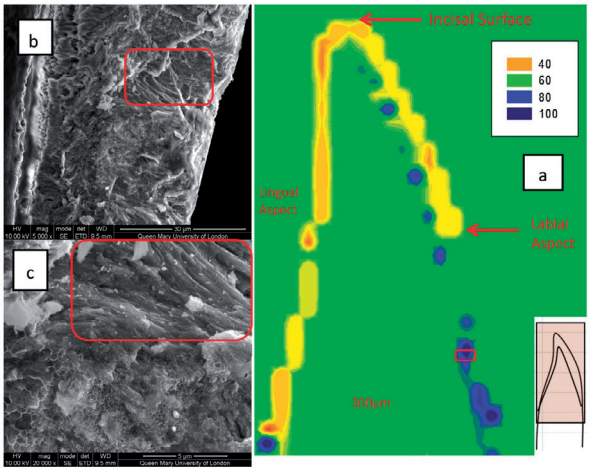

Fig. 11: *MPS IVA affected maxillary central deciduous incisor.* ***(a)*** *Texture map from XRD analysis;* ***(b)*** *SEM of cervical region marked by a red box in the texture map;* ***(c)*** *SEM of the same cervical region at higher magnification.*

X-ray colors for 3D texture scanning

H.C. Lichtenegger, T. Grünewald, W. Bras, H. Rennhofer, L. Vincze, P. Tack, J. Garrevoet – for more information contact H.C. Lichtenegger, Institute of Physics and Materials Science, BOKU Wien, 1090 Vienna, Austria.

helga.lichtenegger@boku.ac.at

A variety of complex materials, most prominently biological tissues such as teeth or bones, are known to exhibit an intricate organisation and preferred orientation of crystallites (crystallographic texture). For many decades, the state of the art texture measurement involved a monochromatic beam and a conventional area detector delivering "grey-scale" diffraction images. True 3D information about crystallite orientation required rotating the sample in the beam and collecting diffraction images at different rotation angles.

We have recently developed a new approach to scan the crystallographic texture of complex materials by using a white beam and exploiting the inherently contained "x-ray colors" to obtain 3D crystallographic information at every point of the sample.

For this purpose, we used a white beam at XMaS and an energy dispersive area detector. The conventional 2-dimensional intensity information was thus complemented by an energy spectrum in each pixel. By using a straightforward algorithm based on the Ewald sphere geometry, the photon energies ("x-ray colors") were used to calculate the missing third dimension in space. In this way a 3D representation of scattering data was achieved without a-priori knowledge of the sample and without the need to rotate the sample.

The example of two crossed strands of carbon fibers is shown in **Fig. 13**. The two orientations are immediately and directly visible from the 3D reconstruction of the scattering image. In lobster tail cuticle, the method revealed a calcite crystal orientation roughly perpendicular to the cuticle plane. At the same time, it also allowed determination of the Ca distribution, since the energy dispersive detector also records the x-ray fluorescence from the sample and thus yields chemical information as well.

In this way, 3D crystallographic and chemical information could be acquired in a single shot, without sample rotation and at a lateral spatial resolution only limited by the beam size. The method is therefore of particular value for fast 2D texture mapping of complex samples or for any setup or system that does not allow rotation. Due to the non-rotational setup and the 3D information it makes the study of correlated effects, e.g. crystallisation and strain development, conceivable. The approach combines the benefits of both, traditional Laue diffraction and monochromatic diffraction, and can therefore be expected to become a powerful and elegant tool in future crystallography, applied chemistry and materials science.

[1] T.A. Grünewald ***et al.***, Angewandte Chemie Int. Ed. 55, 12190 (2016).

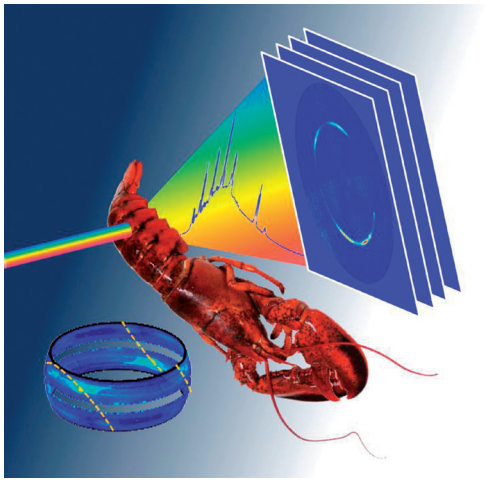

Fig. 12: *Schematic of the white beam texture measurement experiment. The energy dispersive area detector (here visualised as stack of diffraction images) allows 3D texture information at every scan point illuminated by the white beam. Taken from* ***[1]****.*

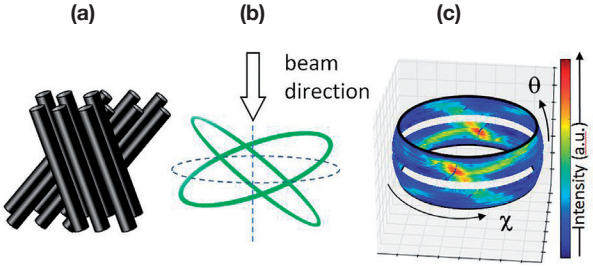

Fig. 13: (a) *Schematic of carbon fibers in crossed orientation.* ***(b)*** *Diffraction rings of (002) reflection from crossed carbon fibers visualised in reciprocal space.* ***(c)*** *3D representation of experimental data, showing immediately the two crossed rings in reciprocal space, thus directly revealing the orientation. Taken from* ***[1]****.*

Nanohybrid shish-kebab structure in PET-MWCNT composites

E.L. Heeley, D.J. Hughes, E.M. Crabb, J. Bowen, O. Bikondoa, B. Mayoral, T. McNally – for more information contact E.L. Heeley or T. McNally, Faculty of Science, Technology, Engineering and Mathematics, Open University, Milton Keynes MK7 6AA or International Institute for Nanocomposites Manufacturing, WMG, University of Warwick, Coventry CV4 7AL, UK.

Ellen.Heeley@open.ac.uk
T.McNally@warwick.ac.uk

The addition of multi-walled carbon nanotubes (MWCNTs) as a filler to poly(ethylene terephthalate) (PET) significantly improves polymer's mechanical and thermal properties **[1,2]**. However, the complex role that MWCNTs play in the crystalline morphology development in polymer composites during processing is still poorly understood. Here, we show the development of a nanohybrid shish-kebab (NHSK) structure in PET-MWCNT composites during hot isothermal crystallisation. The results indicate that MWCNTs act as nucleation points for NHSK-type crystallisation and that the crystalline morphology, which evolves, has a predisposed orientation induced from the initial processing method **[3]**.

Combined SAXS*/WAXS* and thermal techniques were used on XMaS to follow the time resolved morphology development and crystallisation kinetics of the PET-MWCNT composites. SAXS, reveals the crystalline morphology (shish-kebab or regular lamellar) and orientation during the hot isothermal crystallisation process from the melt. WAXS gives information on the polymer crystal lattice. PET-MWCNT composites were prepared via a cast extrusion process **[2]** and referred to by the MWCNT wt% loading PET (e.g. PET1%, PET2% and PET4%). **Fig. 1**, shows 2D SAXS and WAXS of samples extruded at 30 °C. No residual crystalline structure for neat PET is observed in either SAXS or WAXS. In contrast, the PET-MWCNT composites show increased scattering around the beam stop indicative of some residual crystalline content from the extrusion process. PET2% and PET4% composites also show some preferred orientation (arc-like intensity around the beam stop). WAXS for the PET-MWCNT samples shows the crystalline PET triclinic unit cell reflections (010) and (0-11). Final SAXS patterns from the hot isothermal crystallisation process show a random crystalline lamellar structure prevails for neat PET. However, for all the PET-MWCNT composites, a NHSK structure evolves with preferred orientation (as depicted in the final column of **Fig. 14**).

Fig. 15a, shows the change in orientation (FWHM) with increasing crystallisation temperature. Significant orientation is seen in the composites whereas no orientation is seen in neat PET. **Fig. 15b** shows the hot crystallisation curves giving the crystallisation half-times, $t_{1/2}$. The PET-MWCNT composites show increased crystallisation kinetics (reduction in $t_{1/2}$), compared to neat PET, during crystallisation from the melt. Hence, MWCNTs are seen to drastically influence the crystalline morphology of PET, by acting as pre-aligned nucleating agents increasing the crystallisation kinetics of the polymer. This has significant impact on the use of such fillers in the processing and modification of the physical properties of engineering polymers.

[1] E.L. Heeley *et al.*, Polymer 92, 239 (2016).
[2] B. Mayoral *et al.*, RSC Adv. 3, 5162 (2013).
[3] E.L. Heeley *et al.*, J. Polym. Sci. Part B: Polym. 55, 132 (2017).

* See glossary p.5 for definition.

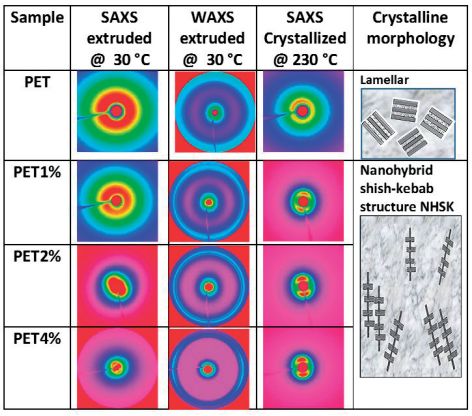

Fig. 14: *2D SAXS and WAXS patterns from extruded samples at 30 °C and SAXS when crystallised at 230 °C. Neat PET shows a random lamellar morphology whereas PET-MWCNT composites show an oriented NHSK morphology.*

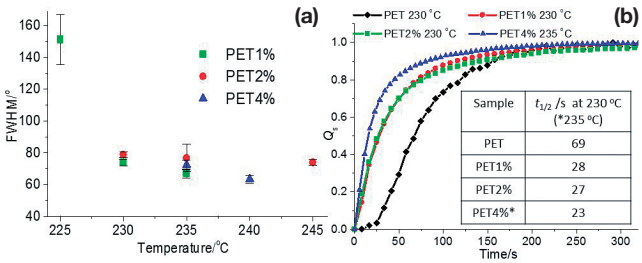

Fig. 15: (a) *Change in orientation full-width half max (FWHM) for PET-MWCNT samples with increasing crystallisation temperature.* ***(b)*** *Selected crystallisation curves – inset table details the crystallisation half-time ($t_{1/2}$).*

Observing IUDs "in-situ"

M.G. Dowsett, R.A. Grayburn, P.-J. Sabbe, and A. Adriaens – for more information contact A. Adriaens, Department of Analytical Chemistry, Ghent University, Krijgslaan 281 S12, B9000 Gent, Belgium.

annemie.adriaens@ugent.be

Copper-bearing intrauterine devices (CuIUDs) are frequently used for long-acting reversible contraception. The release of copper ions into the fluid medium of the uterus reduces the probability of ovum fertilisation and endometrial adhesion. It is widely believed that the primary source of these ions is cuprite (Cu_2O) formed on the device surface through in-utero corrosion. However, cuprite has a very low solubility at the pH and temperature of the uterine fluid so this seems unlikely, especially when far more soluble compounds such as copper sulphate and chloride may also be formed.

Further development of the CuIUD involves exploiting geometries with a high surface area to volume ratio compared to the traditional "coil" combined with enhanced copper dissolution, e.g. through exploiting galvanic corrosion. However, the interactions between the copper and the uterine fluid need to be better understood.

We studied the surface reaction products *in-situ* using XRD* on XMaS **[1]** with a custom made portable electrochemical cell (peCell), filled with simulated uterine fluid (**Fig. 16**). Copper coupons with three levels of partial gold coating (1.4%, 5% and 25% by area) were studied simultaneously to assess the influence of galvanic corrosion. Our approach is intended to eliminate misleading results from *in-utero* samples subjected to removal, cleaning and storage prior to analysis. This may cause insoluble crusts to be formed. The new peCell allowed us to follow the surface changes over 8 consecutive days. However, as it is both portable and designed to maintain conditions indefinitely, longer term experiments are possible in the future.

Over a period of 8 days, copper with less than 25% coverage of gold became coated with Cu_2O and released colloidal Cu_2S into the fluid. Neither of these compounds is likely to promote anticonception as they are both insoluble at the uterine pH and temperature. Crystalline NaCl was also deposited from the fluid. The surfaces and the fluid became visibly blackened.

Surface CuCl and CuS (both insoluble) were also observed for the lowest gold coverage. (CuCl reacts with water to form Cu_2O and with water vapour in the air to form $Cu_2(OH)_3Cl$ and so can distort the results from rinsed and stored samples analysed *ex-situ*). The sample with 25% gold coverage showed little formation of insoluble products although CuO and CuS were present. However, a crystalline phase of $CuCl_2$ became visible to XRD after around 7 days. This is extremely soluble under *in-vivo* conditions and the fact that it was observed as a solid indicates a high rate of production at the surface. The XRD will not see products which are in solution, but the release of Cu++ ions likely takes place through reaction with chlorine naturally present in uterine fluid and in our simulant, as indicated by the results from the highest gold coverage.

Partial gold coating strongly modifies the behaviour of the copper in the simulated uterine environment in an area dependent way and, for sufficiently large areas, appears to drive the reactions to form more soluble compounds therefore putting more copper in solution. Longer term experiments using synchrotron XRD of the surface and XAS* of the fluid will be carried out to verify and extend these results with the objective of further improving frameless intrauterine devices.

[1] R.A. Grayburn *et al.*, Bioelectrochemistry 110, 41 (2016).

* See glossary p.5 for definition.

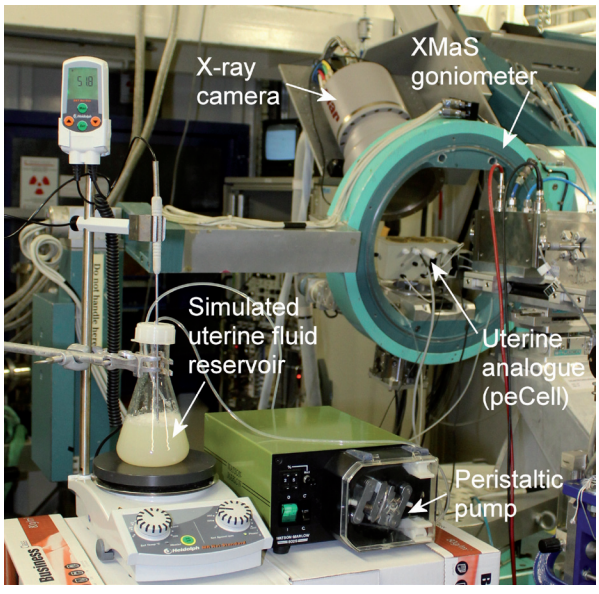

Fig. 16: *Portable electrochemical/environmental cell (peCell) containing copper coupons part-coated with gold in circulating simulated uterine fluid.*

Li-S battery – PANI binder prevents long chain polysulphide formation

N. Yokota, F. Ooms, M.P. Hogan, A. Blidberg, P. Thompson, E. Kelder, M.L. Alfredsson – for more information contact N. Yokota, School of Physical Sciences, University of Kent, Canterbury CT2 7NY, UK.

Ny39@kent.ac.uk

Lithium Sulphur (Li-S) batteries are considered as one of the most promising candidate to replace current Lithium ion battery materials due to its high theoretical energy density at much lower cost **[1]**. However, the commercial application of Li-S batteries are still not capable due to many problematic issues including poor cyclebility and rapid capacity decay caused by polysulfide shuttle reaction **[2]**.

During Li-S battery cycling, sulphur is reduced and yields polysulphide intermediates. There are two different types of polysulphides such as highly soluble long chain polysulphide Li_2S_X ($4<x\leq8$) and insoluble short chain polysulphide Li_2S_X ($2<x\leq4$). Long chain polysulphides are formed at the initial stage of battery discharge and dissolve into the electrolyte. These migrate and accumulate on the lithium anode side, resulting in loss of active sulphur from the cathode and reduce the capacity of the cell **[3]**. Although extensive research has been conducted, the mechanism of these problems is not fully understood yet.

It was discovered that *in-situ* XAS* is a powerful tool to gain better understanding of sulphur transformation to polysulphides during Li-S battery cycling **[4]**. This work conducted at XMaS has enabled us to investigate the local structures of sulphur in different cathode compositions, comparing two different types of polymer binders, polyaniline (PANI) and PEDOT:PSS. A previous galvanostatic study proved that PEDOT:PSS is a better conductive binder to extend the cycle life of Li-S battery than PANI **[5]**. *In-operando* XAS measurement was carried out to determine the polysulphide formation in detail. **Fig. 17** displays the construction of the *in-situ* coin cell. The XANES* spectrum of a typical S K-edge of polysulphide (**Fig. 18**) shows the pre-edge contribution from the terminal sulphur atoms and main edge attributed to the internal sulphur atoms. Transition of the sulphur to polysulphides during battery cycling was measured based on the area ratio and energy shift of these two peaks.

It was discovered that PANI coating of sulphur particles effectively prevents the formation of long chain Li_2SX polysulphides and instead directly transforms cyclo-S_8 into short chain polysulphides reducing the shuttle reaction.

[1] S.S. Zhang, J. Power. Sour 231, 153 (2013).
[2] L. Nazar, J. Mater. Chem. 20, 9821 (2010).
[3] J.Guo *et al.*, Nano Lett. 11, 4288 (2011).
[4] D. Robert *et al.*, J. Phys. Chem. 119, 19001 (2015).
[5] L. Weiyang *et al.*, Nano Lett. 13, 5534 (2013).

* See glossary p.5 for definition.

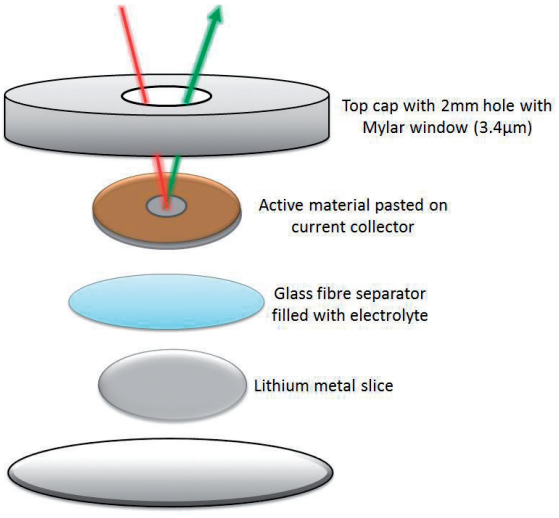

Fig. 17: In-situ *coin cell construction.*

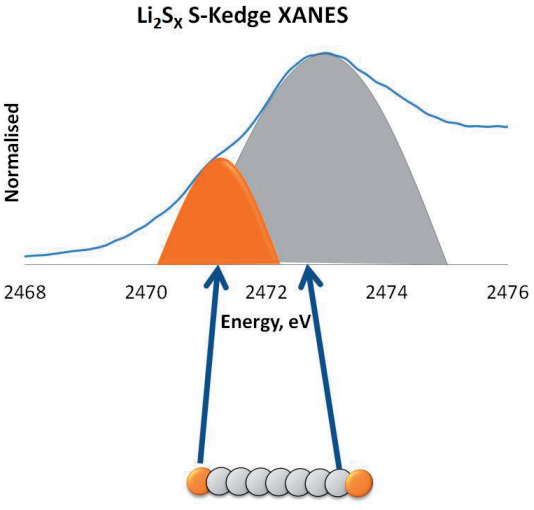

Fig. 18: *Determination of internal and terminal sulphur of polysulphides.*

➡ Please note

Some of the experimental reports in the previous pages are as yet unpublished. Please email the contact person if you are interested in any of them or wish to quote these results elsewhere.

➡ Our web site

This can be found at: **www.xmas.ac.uk** and contains the definitive information about the beamline, future and past workshops, press articles, Key Performance Indicators (KPIs). You can also follow what happens on the beamline every week on **Twitter@XMaSBeam**

➡ Living allowances

These are € 70 per day per beamline user — the equivalent actually reimbursed in pounds sterling. XMaS will support up to 3 users per experiment. For experiments which are user intensive, additional support may be available. The ESRF hostel still appears adequate to accommodate all our users, though CRG users will always have a lower priority than the ESRF's own users. Do remember to complete the "A-form" when requested to by the ESRF, as this is used for hostel bookings, site passes and to inform the safety group of attendees.

➡ Beamline people

- **Beamline Responsible –** Didier Wermeille (didier.wermeille@esrf.fr), in partnership with the Directors, oversees the activities of the user communities as well as the programmes and developments that are performed on the beamline. He is also the beamline Safety Representative.
- **Beamline Coordinator –** Laurence Bouchenoire, (bouchenoire@esrf.fr), looks after beamline operations and can provide you with general information about the beamline, application procedures, scheduling, etc. Laurence should normally be your first point of contact.
- **Beamline Scientists –** Didier Wermeille (didier.wermeille@esrf.fr), Oier Bikondoa (oier.bikondoa@esrf.fr), Simon Brown (sbrown@esrf.fr) and Laurence Bouchenoire (bouchenoire@esrf.fr) are Beamline Scientists and will provide local contact support during experiments. They can also assist with queries regarding data analysis and software.
- **Technical Support –** Paul Thompson (pthompso@esrf.fr) is the contact for instrument development and technical support. He is assisted by John Kervin (jkervin@liv.ac.uk), who is based at Liverpool University. He provides further technical back-up and spends part of his time on-site at XMaS.
- **Project Directors –** Chris Lucas (clucas@liv.ac.uk) and Tom Hase (t.p.a.hase@warwick.ac.uk) continue to travel between the UK and France to oversee the operation of the beamline. Malcolm Cooper (m.j.cooper@warwick.ac.uk) remains involved in the beamline operation as an Emeritus Professor at the University of Warwick. Kayleigh Lampard (Kayleigh.Lampard@warwick.ac.uk) is the principal administrator on the project and is based in the Department of Physics at Warwick. All queries regarding expenses claims, etc. should be directed to her. Linda Fielding (linda.fielding@liv.ac.uk) is the administrator at the University of Liverpool.

The Project Management Committee

The current membership of the committee is as follows:

- P. Hatton (chair), University of Durham
- S. Crook, EPSRC
- S. Beaufoy, University of Warwick
- A. Boothroyd, University of Oxford
- M. Cain. Electrosciences Ltd
- R. Cernik, University of Manchester
- K. Edler, University of Bath
- B. Hickey, University of Leeds
- S. Langridge, ISIS, Rutherford Appleton Laboratoy
- C. Nicklin, Diamond Light Source
- W. Stirling, Institut Laue Langevin

in addition to the above, the directors, the chair of the PRP, the CRG Liaison Engineer A. Kaprolat and the beamline team are in attendance at the meetings which happen twice a year.

➡ The Peer Review Panel

The current membership of the panel is as follows:

- R. Johnson (chair), University of Oxford
- E. Blackburn, University of Birmingham
- W. Briscoe, University of Bristol
- S. Corr, University of Glasgow
- C. Detlefs, ESRF
- Y. Gründer, University of Liverpool
- J. Quintanilla, University of Kent
- R. Walton, University of Warwick
- J. Webster, STFC

In addition either Chris Lucas or Tom Hase attends the meetings in an advisory role.

➡ Housekeeping!!

At the end of your experiment samples should be removed, tools, etc. returned to racks and unwanted materials disposed of in appropriately. When travel arrangements are made, therefore, please allow additional time to effect a tidy-up.

➡ PUBLISH PLEASE!!… and keep us informed

Although the list of XMaS papers is growing we still need more of those publications to appear. We ask you to provide Kayleigh Lampard with the reference. You can also submit the reference of your new publication directly from our web site (www.xmas.ac.uk/impact/publications/publication_submission/).

➡ IMPORTANT!

It is important that we acknowledge the support from EPSRC in any publications. When beamline staff have made a significant contribution to your scientific investigation you may naturally want to include them as authors. Otherwise we ask that you add an acknowledgement, of the form:

"XMaS is a mid-range facility supported by EPSRC. We are grateful to all the beam line team staff for their support."

How to apply for synchrotron beam time ?

➡ Beamline Operation

The XMaS beamline at the ESRF, which came into operation in April 1998, has some 174 days of synchrotron beam time available each year for UK user experiments, after deducting time allocated for ESRF users, machine dedicated runs and maintenance days. During the year, two long shut-downs of the ESRF are planned: 4 weeks in winter and 4 weeks in summer. At the ESRF, beam is available for user experiments 24 hours a day.

➡ Applications for Beam Time

Two proposal review rounds are held each year. **Deadlines for applications to make use of the mid-range facility (CRG) time are normally, 1st April and 1st October** for the scheduling periods August to end of February, and March to July, respectively. Applications for Beam Time must be submitted electronically following the successful model used by the ESRF. Please consult the instructions given in the ESRF web page:

www.esrf.eu

Follow the links **"User Portal"** under **"quick links"**.
Enter your surname and password
and select: **"Proposals/Experiments"**.

Follow the instructions carefully — you must choose "CRG Proposal" and "XMAS-BM28" at the appropriate stage in the process. A detailed description of the process is always included in the reminder that is emailed to our users shortly before the deadline – for any problems contact Laurence Bouchenoire (bouchenoire@esrf.fr). Technical specifications of the beamline and instrumentation available are described in the XMaS web page (www.xmas.ac.uk).

■ When preparing your application, please consider that access to the mid-range facility time is only for UK based researchers. Collaborations with EU and international colleagues are encouraged, but the proposal must be lead by a UK based principal investigator and it must be made clear how the collaborative research supports the UK science base. Applications without a robust link to the UK will be rejected and should instead be submitted directly to the ESRF.

■ All sections of the form must be filled in. Particular attention should be given to the safety aspects, and the name and characteristics of the substance completed carefully. Experimental conditions requiring special safety precautions such as the use of electric fields, lasers, high pressure cells, dangerous substances, toxic substances and radioactive materials, must be clearly stated in the proposal. Moreover, any ancillary equipment supplied by the user must conform to the appropriate French regulations. Further information may be obtained from Martine Moroni, the ESRF Experimental Safety Officer for CRG beamlines (martine.moroni@esrf.fr, tel: +33 (0)4 76 88 23 69).

■ Please indicate your date preferences, including any dates that you would be unable to attend if invited for an experiment. This will help us to produce a schedule that is satisfactory for all.

■ An experimental report on previous measurements must be submitted. **Applications will not be considered unless a report on previous work is submitted.** These also should be submitted electronically, following the ESRF model. The procedure for the submission follows that for the submission of proposals — again, follow the instructions in the ESRF's web pages carefully. **Reports must be submitted within 6 months of the experiment.** Note that the abstract of a publication can also serve as the experimental report! Please also remember to fill in the end of run survey form on completin of your experiment, which is available on the website.

■ The XMaS beamline is available for one third of its operational time to the ESRF's user community. Applications for beamtime within that quota should be made in the **ESRF's proposal round** - Note: their **deadlines** are earlier than for XMaS! - **1st March and 10th September.** Applications for the same experiment may be made both to XMaS directly and to the ESRF. Obviously, proposals successfully awarded beamtime by the ESRF will not then be given beamtime additionally in the XMaS allocation.

➡ Assessment of Applications

The Peer Review Panel considers the proposals, grades them according to scientific excellence, adjusts the requested beam time if required, and recommends proposals to be allocated beam time on the beamline. Proposals which are allocated beam time must in addition meet ESRF safety and XMaS technical feasibility requirements. Following each meeting of the Peer Review Panel, proposers will be informed of the decisions taken and some feedback provided.

is an EPSRC sponsored project

XMaS, ESRF – The European Synchrotron, CS 40220, 38043 Grenoble Cedex 9, France
Tel: +33 (0)4 76 88 25 80 – web page : www.xmas.ac.uk – email: bouchenoire@esrf.fr

Editor: Laurence Bouchenoire – Layout: J.C. Irma-BNPSI – Print: WarwickPrint – January 2017